

Inflation: Observations and Attractors

Diederik Roest and Marco Scalisi

Abstract In these lecture notes, we present the latest status of CMB observations and outline a particular set of inflationary models to explain these data. As an introduction, we provide the necessary background to understand the Planck results on the temperature fluctuations of the CMB. We then explain how these results can be interpreted in terms of the number of e-folds during inflation. Finally, we discuss theoretical models that underpin this interpretation and yield robust predictions for future CMB observables.

1 Introduction and Outline

These notes are an extended write-up of a set of lectures given by the first author in the school “Theoretical Frontiers in Black Holes and Cosmology” in Natal, Brazil, from June 8–12, 2015. They do not aim to give an exhaustive overview of cosmological inflation; instead we will highlight a number of recent developments, both at the observational as well as theoretical front, with an interesting interplay between them. We hope they serve as an interesting stand-alone introduction to these particular aspects of inflation. When possible we will avoid technical details, deferring these to the original literature, and take a more pedestrian approach.

We will first introduce the standard cosmological viewpoint. This leads one to conjecture a period of inflation in the very early Universe. In order to understand the consequences of this phase, we study a consistent quantum formulation of the paradigm where initial quantum fluctuations represent the natural seeds for the formation of the cosmological structures. This allows us to present the most recent observations on the cosmic microwave background, and provide a theoretical interpretation

D. Roest (✉) · M. Scalisi

Van Swinderen Institute for Particle Physics and Gravity, University of Groningen,
Nijenborgh 4, 9747 AG Groningen, The Netherlands
e-mail: d.roest@rug.nl

M. Scalisi
e-mail: m.scalisi@rug.nl

of them. Finally, we discuss progress in inflationary model building, focusing on the notion of cosmological attractors. Throughout these notes we will refer to some of the relevant papers. Complementary material can be found in more extensive reviews, see e.g. [1–5]

2 Standard Cosmology in a Nutshell

In 1929 the astronomer Edwin Hubble made a discovery [6] which has revolutionized the understanding of our Universe as a whole, and has given rise to the subsequent establishment of cosmology as a science. He observed the mutual recession of galaxies, which was almost immediately interpreted as first evidence that we live in an expanding Universe. This simple idea led to the development of the standard model of Big Bang cosmology, whose predictions are in excellent agreement with observations. Despite the name, the model says nothing about the “Big Bang” which remains a mathematical singularity as well as an unsolved physical question. On the other hand, it furnishes a clear and precise picture of the cosmic evolution from a few seconds after this mysterious start: the temperature decreases as the expansion of the Universe proceeds, light elements form during a process called Big Bang Nucleosynthesis (BBN), recombination of nuclei and electrons takes place followed by the last scattering of photons which freely reach us today as cosmic microwave background (CMB) radiation, observed in the sky at the temperature $T = 2.73$ K.

Although the model has had many successful experimental confirmations, it contains some serious theoretical shortcomings which can be better understood once we know the geometric properties of the Universe we live in.

2.1 FRW Geometry and Dynamics

A dynamical Universe is what comes naturally from Einstein theory of general relativity which relates the geometry of spacetime to its matter-energy content, through the field equations (throughout these notes we have fixed Newton’s constant by setting the reduced Planck mass to unity: $M_{Pl} = 1$)

$$G_{\mu\nu} = T_{\mu\nu}. \quad (1)$$

Prior to Hubble’s discovery, Einstein had already noticed such a genuine prediction of a non-static Universe. However, puzzled by its cosmological implications, he augmented his equations with a specific cosmological constant in order to avoid such a phenomenon. Hubble’s discovery however confirmed that we do live in a non-static Universe.

The simple observation that our Universe is homogeneous and isotropic at large scales (> 100 Mpc) imposes stringent constraints on the form of both sides of (1).

Originally an assumption, this so-called *cosmological principle* has been beautifully confirmed by the observations of the distribution of galaxies at large scales REF and the homogeneity and isotropy of the CMB radiation REF. Assuming these symmetries leads to the Friedmann–Robertson–Walker (FRW) metric which, written in terms of polar spherical coordinates (r, θ, σ) , reads

$$ds^2 = -dt^2 + a(t)^2 \left[\frac{dr^2}{1 - r^2} + r^2(d\theta^2 + \sin^2 \theta d\sigma^2) \right]. \tag{2}$$

The scale factor $a(t)$ sets the physical distances among objects and can vary with respect to the cosmic time t (the proper time as measured by a comoving observer at constant spatial coordinates) allowing, then, for an expanding Universe. The coordinates (r, θ, σ) reflect the symmetries assumed and are called “comoving coordinates” as they are decoupled from the effect of the expansion. An FRW Universe can be thought as an expanding grid where objects can be fixed on it (i.e. at constant comoving coordinates) and still recede from each other as an effect of a growing scale factor. Typical scales, e.g. the wavelength λ of a photon, will increase as $\lambda \propto a$ as the expansion proceeds. However, the comoving wavelength λ/a will remain constant in time, if no other external process occurs (see Fig. 1).

Homogeneity and isotropy still allow for a constant curvature of the 3-dimensional spatial slices which can correspond to an open, flat or closed Universe and is parametrized by $\kappa = -1, 0, 1$, respectively. Moreover, the stress-energy tensor $T_{\mu\nu}$, compatible with such symmetries, is the one of a perfect fluid, that is

$$T^\mu{}_\nu = \text{diag}(-\rho, p, p, p), \tag{3}$$

where ρ is the energy density and p the pressure as measured in the rest frame of the fluid.

Due to the symmetries assumed, the independent equations (1) turn out to be two which are known as *Friedmann equations* and read

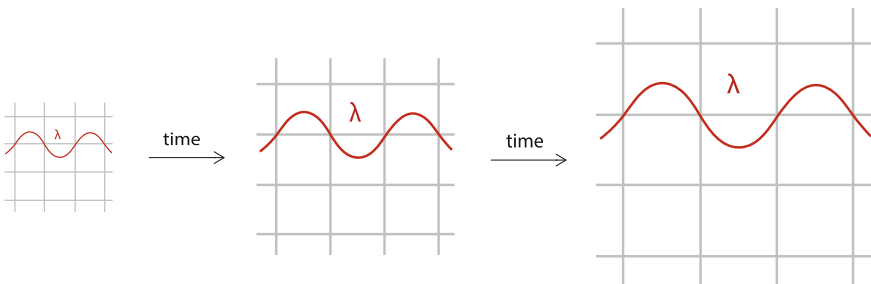


Fig. 1 The expanding Universe with a typical scale λ . The grid schematically represents comoving coordinates which do not change with time. Physical distances increase proportionally with the scale factor $a(t)$

$$H^2 = \frac{\rho}{3} - \frac{\kappa}{a^2}, \quad \frac{\ddot{a}}{a} = -\frac{1}{6}(\rho + 3p), \quad (4)$$

where dots denote derivatives with respect to the time t and we have defined the Hubble parameter as

$$H \equiv \frac{\dot{a}}{a}. \quad (5)$$

In order to extract the evolution of the scale factor $a(t)$, one must specify the type of matter and solve (4). In fact, these two equations can be combined into the continuity equation

$$\dot{\rho} + 3H(\rho + p) = 0, \quad (6)$$

which, alternatively, can be also derived from the condition of energy conservation $\nabla_{\mu} T^{\mu\nu} = 0$. Depending on the relation between energy density and pressure, dictated by the equation of state parameter

$$p = w\rho, \quad (7)$$

we obtain the following scaling for the energy density

$$\rho \propto a^{-3(1+w)}, \quad (8)$$

which, plugged back into (4), yields

$$a(t) \propto \begin{cases} t^{\frac{2}{3(1+w)}}, & w \neq -1 \\ e^{Ht}, & w = -1 \end{cases} \quad (9)$$

in the case of flat curvature ($\kappa = 0$). The parameter w can be assumed to be constant and depends on the specific species filling the Universe at any epoch:

- *Radiation*, or any species with dominating kinetic energy (e.g. photons or neutrinos), is characterized by $w = 1/3$. The energy density scales as $\rho \propto a^{-4}$ which implies that a Universe dominated by such type of matter expands as $a \propto t^{1/2}$.
- *Matter*, or any pressure-less species where kinetic energy is negligible with respect to the mass (e.g. baryons or dark matter), is characterized by $w = 0$. One has $\rho \propto a^{-3}$ and a Universe dominated by matter will have a scaling $a \propto t^{2/3}$.
- *Dark energy*, the mysterious component dominating the Universe nowadays, is characterized by $w = -1$ (when described by a cosmological constant) with negative pressure and constant energy density. A Universe dominated by that will expand exponentially as given by (9).

In standard cosmology, therefore, the history of the Universe is characterized by early times dominated by radiation, a moment of matter-radiation equality and subsequent domination of matter. Just recently we have entered an era in which dark

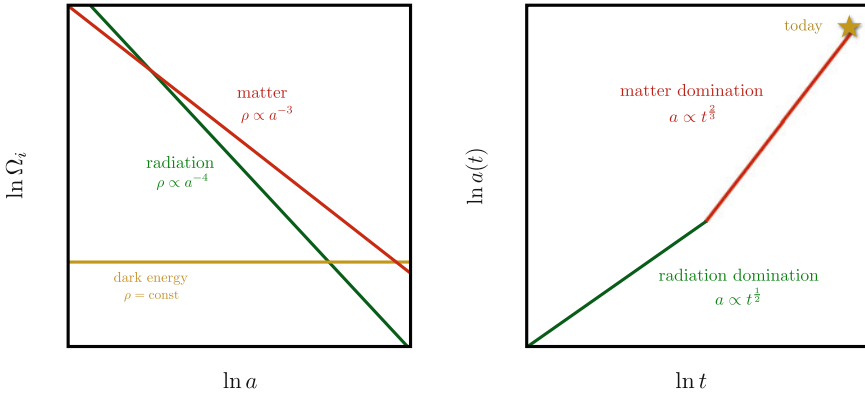


Fig. 2 Standard evolution of the energy densities (*left panel*) and the scale factor (*right panel*). According to the standard cosmological model, going back in time, the Universe becomes radiation dominated and the scale factor shrinks up to a singular point $a = 0$, commonly called “Big Bang”

energy constitutes most of the total energy in the Universe, at present 68.3% of the entire content. This evolution is shown in Fig. 2.

Finally, one may write the Friedmann equation in a form which is better for the discussion of the shortcomings affecting the standard cosmological model. By looking at (4), one may define, at any time, a critical energy density

$$\rho_c \equiv 3H^2 \tag{10}$$

corresponding to a perfect flat sectional curvature $\kappa = 0$. After normalizing all energy densities as

$$\Omega_i \equiv \frac{\rho_i}{\rho_c}, \tag{11}$$

one can rewrite (4) as

$$\Omega \equiv \sum_i \Omega_i = 1 + \frac{\kappa}{(aH)^2}. \tag{12}$$

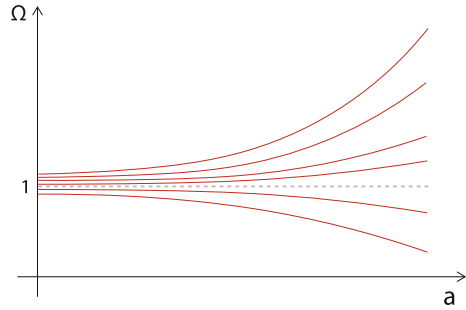
2.2 Flatness Problem

In standard cosmology, an expanding Universe is naturally driven away from flatness. This can be well understood by differentiating (12), that is

$$\dot{\Omega} = H\Omega(\Omega - 1)(1 + 3w), \tag{13}$$

which can be rewritten as

Fig. 3 Evolution of the total energy density in standard cosmology. The point $\Omega = 1$, corresponding to flat curvature, is a repeller



$$\frac{d|\Omega - 1|}{d \ln a} = \Omega |\Omega - 1| (1 + 3w). \quad (14)$$

A Universe with a growing scale factor $a(t)$ that is dominated by ordinary matter (subject to the strong energy condition $1 + 3w \geq 0$) therefore has $\Omega = 1$ as an unstable fixed point as displayed in Fig. 3.

This is exactly what happens in the standard cosmological picture where the Universe has been dominated by such type of energy from the beginning until the present time, as shown in Fig. 2. A Universe starting with generic initial curvature is driven away from flatness during its evolution. The same conclusion can be reached by looking at (12) and noticing that, in a Universe filled with radiation or matter, the sum of the energy densities Ω_i diverges from unity as the quantity $(aH)^{-1}$ increases with time.

The surprise comes with cosmological observations that suggest that the Universe today must be flat with an accuracy of 10^{-2} . This implies that, going back in time, the curvature of the Universe should have been even closer to perfect flatness: at the BBN epoch $|\Omega - 1| \lesssim 10^{-16}$, at the Planck scale $|\Omega - 1| \lesssim 10^{-64}$. Generally, such an incredible amount of fine-tuning for the initial conditions of the Universe makes physicists uncomfortable. A dynamical explanation of what we observe today would be certainly more desirable.

2.3 Horizon Problem

Given a space–time, the scale of causal physics is set by null geodesics, being the paths of photons. In an FRW Universe, with flat curvature, radial null geodesics (i.e. at constant θ and ϕ) are defined as

$$ds^2 = -dt^2 + a(t)^2 dr^2 = 0 \quad \Rightarrow \quad dr = \pm \frac{dt}{a(t)} \equiv \pm d\tau \quad (15)$$

where, in the last step, we have introduced the *conformal time* τ which simplifies the description of the causal structure of the FRW metric: the propagation of light is the same as in Minkowski space and take place diagonally (at 45°) in the (r, τ) plane.

If we assume the standard picture given by Fig. 2, the Universe was dominated by ordinary matter with state parameter $w > -1/3$ for most of its evolution and, going back in time, the scale factor $a(t)$ decreases up to the singular point $a(0) = 0$. In this case there is a maximum distance to which an observer, at time t_0 , can see a light-signal sent at $t = 0$. In comoving coordinates, this is given by the so-called *comoving particle horizon*, that is

$$r_{ph} = \int_0^{t_0} \frac{dt}{a(t)} = \int_0^{a_0} (aH)^{-1} da. \quad (16)$$

If the comoving distance between two particles is greater than r_{ph} , they could have never talked to each other. Assuming (9) and integrating (16), we get

$$r_{ph} \sim a_0^{\frac{1}{2}(1+3w)} \sim (a_0 H_0)^{-1}. \quad (17)$$

Then, in an expanding Universe filled with ordinary matter, the horizon grows with time which means that comoving scales entering the horizon today have been never in causal contact before, as shown in Fig. 2.

The quantity $(aH)^{-1}$ is called *comoving Hubble radius* and determines the distance over which one cannot communicate at a given time. It basically fixes the causal structure of the space–time and its time-evolution is crucial for the particle horizon in (16).

3 Inflation

The shortcomings of standard cosmology concern the initial conditions of our Universe that require serious fine-tuning in order to reproduce what we observe today. The flatness problem can be solved by assuming that the initial value of the curvature was precisely flat. Similarly, in order to solve the horizon problem, one should imagine at least 10^6 causally disconnected spatial patches to have started their evolution exactly in the same physical conditions, in particular at the same temperature and same magnitude of perturbations. Postulating all this is possible but hardly attractive to a physicist that aims to understand the very early Universe.

In order to do better, inflation was proposed in the 1980s [7–9] to solve these problems all at once. The fundamental idea is that the primordial Universe underwent a finite phase of quasi-exponential expansion (similar to the one we are experiencing nowadays with dark energy) which changed the causal structure and how information propagates. As a bonus, one gets a physical mechanism to explain the presence of very small inhomogeneities as quantum fluctuations in the very early Universe; ultimately, these represent the seeds for the large scale structures we observe in the sky.

3.1 Basic Idea

Standard cosmology assumes that the early Universe was dominated by some form of energy satisfying the strong energy condition $\rho + 3p \geq 0$ which implies a decelerating phase of the scale factor, $\ddot{a} < 0$, as dictated by (4). This is at the core of both the flatness and horizon problems.

Inflation is nothing but inverting such a behavior and postulating a phase of accelerated expansion such as

$$\ddot{a} > 0, \quad (18)$$

which implies that the Universe was filled with some kind of matter with negative pressure, satisfying

$$\rho + 3p < 0. \quad (19)$$

The idea that, at very early times, neither matter nor radiation represented the dominant components of energy is not in contrast with any well-tested physical theory. In fact, the standard model of particles physics (SM) cannot be assumed to work up to the first moments after the Big Bang, when energies were several orders of magnitude higher than the domain of validity of the SM (which extends up to around one TeV). Inflation lives off the idea that something non-trivial might have happened due to high-energy physics.

3.2 Decreasing Hubble Radius

Interestingly, the condition (18) turns out to be equivalent to a decreasing comoving Hubble radius

$$\frac{d}{dt}(aH)^{-1} < 0, \quad (20)$$

which gives a deeper insight into the causal structure of a Universe undergoing a phase of inflationary expansion. Typical scales, being initially inside the horizon, leaves the radius of causal contact as inflation proceeds and the Hubble radius $(aH)^{-1}$ decreases. They start reentering the horizon when inflation ends, the standard cosmological evolution progresses and $(aH)^{-1}$ increases. This situation is illustrated in Fig. 4.

The horizon problem is solved if one allows for enough inflation such that also the largest scales we observe in the sky today (CMB and LSS scales) were inside the horizon at early times. Then, the CMB photons had enough time to exchange information and thermalize. Quantitatively, this means that the comoving scales of the observable Universe today $(a_0 H_0)^{-1}$ must fit inside the comoving Hubble radius at the beginning of inflation $(a_i H_i)^{-1}$, that is

$$(a_i H_i)^{-1} > (a_0 H_0)^{-1}. \quad (21)$$

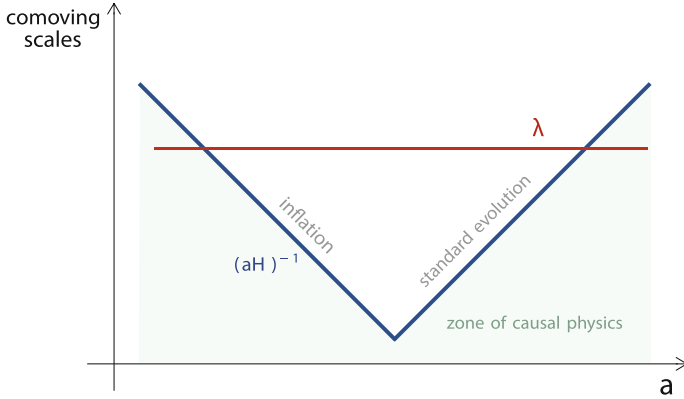


Fig. 4 The Hubble and a typical comoving scale as a function of the scale factor. Due to the anomalous scaling of the comoving Hubble radius, which does not remain constant in time as it happens for all typical scales, the zone of causal physics change with time

The amount of inflation needed to allow for this resolution is quantified by the number of e-folds N :

$$e^N = \frac{a_{\text{end}}}{a_i}, \tag{22}$$

determined by the increase of the scale factor during inflation. A number $N \gtrsim 50-60$ suffices to explain the thermalization of the largest observational scales at present.

The flatness problem is overcome by means of the same mechanism. A decreasing comoving Hubble radius $(aH)^{-1}$ drives the value of the total energy density Ω to unity, providing a physical explanation for this apparently fine-tuned configuration. After inflation, the curvature will start diverging from $\Omega \approx 1$, as it happens in a Universe filled with ordinary matter. Interestingly, the same amount of inflation needed to solve the horizon problem is enough to explain the flatness we observe today. In fact, during inflation we have

$$\Omega - 1 = \frac{k^2}{(aH)^2} \propto e^{-2N} \rightarrow 0. \tag{23}$$

The same number of e-folds quoted before would give the accuracy required for the value observed today.

3.3 Scalar Field Dynamics and Slow-Roll Inflation

The Einstein equations tell us that inflation should be supported by some form of matter with a negative pressure, as given by (19). However, we are still left with the

issue of identifying the origin of such an incredible energy which led the scale factor to increase by an order of 10^{28} .

The simplest example is to imagine that (a small portion of) the primordial Universe is filled with a scalar field, often called *inflation* field, minimally coupled to gravity with Lagrangian

$$\mathcal{L} = \sqrt{-g} \left[\frac{1}{2}R - \frac{1}{2}g^{\mu\nu} \partial_\mu \phi \partial_\nu \phi - V(\phi) \right], \quad (24)$$

leading to the energy-momentum tensor

$$T_{\mu\nu} = \partial_\mu \phi \partial_\nu \phi - g_{\mu\nu} \left[\frac{1}{2} \partial^\sigma \phi \partial_\sigma \phi + V(\phi) \right]. \quad (25)$$

In the case of a homogeneous scalar field $\phi(t)$ filling a patch of the Universe with flat FRW metric (2), the energy density and pressure turn out to be simply

$$\rho \equiv T_{00} = \frac{1}{2} \dot{\phi}^2 + V(\phi), \quad p \equiv T_{ii} = \frac{1}{2} \dot{\phi}^2 - V(\phi). \quad (26)$$

The dynamics and interaction of the spacetime metric and scalar field is described by the two equations

$$H^2 = \frac{1}{3} \left[\frac{\dot{\phi}^2}{2} + V(\phi) \right], \quad \ddot{\phi} + 3H\dot{\phi} + V' = 0, \quad (27)$$

where primes denote derivatives with respect to ϕ . The first is simply the Friedmann equation (4), with $\kappa = 0$. The second is the equation of motion for the scalar field which is derived by varying its action. It describes a particle rolling down along its potential and subject to a friction due to the expansion term $3H\dot{\phi}$.

This region of the Universe will inflate if the state parameter $w = p/\rho < -1/3$, which is easily realizable if the potential energy dominates over the kinetic energy, that is

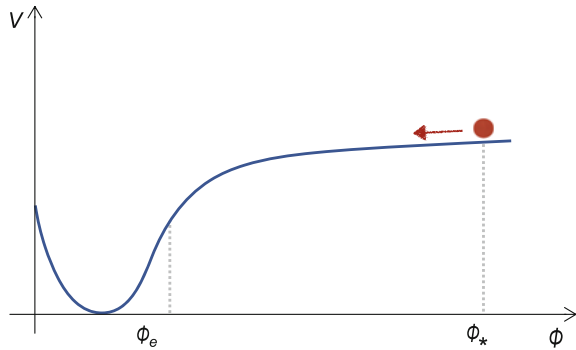
$$V(\phi) \gg \dot{\phi}^2. \quad (28)$$

The regime described by (28) is said *slow-roll inflation* as the field will evolve really slowly with respect to the quasi-exponential growth of the scale factor. Further, in order to have an inflationary period lasting long enough, one must ensure a small acceleration of the field and therefore impose

$$|\ddot{\phi}| \ll |3H\dot{\phi}|. \quad (29)$$

Intuitively, such a scenario is possible any time that the shape of the potential is sufficiently flat (in some measure) as it is shown in the cartoon of Fig. 5.

Fig. 5 Cartoon picture of a typical inflationary potential. The scalar field slowly rolls down along the shape driving the quasi-exponential expansion. Inflation ends at ϕ_e and starts at ϕ_* , at least around 60 e-foldings before the end



Within the slow-roll regime, the dynamical equations (27) become

$$H^2 \approx \frac{V(\phi)}{3} \approx \text{constant}, \quad \dot{\phi} \approx -\frac{V'}{3H}. \tag{30}$$

Given a scalar field with its potential $V(\phi)$, one can verify whether such scenario is suitable for inflation or not by calculating the so-called *slow-roll parameters*, defined as

$$\varepsilon \equiv \frac{1}{2} \left(\frac{V'}{V} \right)^2, \quad \eta \equiv \frac{V''}{V}, \tag{31}$$

and check that

$$\{\varepsilon, |\eta|\} \ll 1, \tag{32}$$

which is equivalent to (28) and (29).

Eventually, inflation must end and give way to the standard cosmological evolution (with an increasing Hubble radius and ordinary matter domination). This happens when the conditions (32) are violated: the trajectory becomes first too steep and the inflaton eventually falls into a local minimum. The oscillations around the vacuum convert the inflationary energy into ordinary particles, within a process called *reheating*.

4 Quantum to Classical Perturbations

4.1 The Inhomogeneous Universe

The inflationary paradigm elegantly solves the standard cosmological puzzles, providing a natural explanation for the homogeneity and isotropy at large distances. However, at scales smaller than 100Mpc, we do observe structures in form of

galaxies, stars and so on. The standard cosmological theory allows us to accurately trace the evolution of such structures back in time. We are able to identify their origin in the gravitational instability of small density perturbations of a primordial plasma made up of photons and baryons, which have evolved into the large-scale structures of the present Universe.

This idea of structure formation is confirmed by the oldest snapshot we have of our Universe: the cosmic microwave background (CMB). It was produced at the time when electrons and nuclei have just recombined, around 300,000 years after the Big Bang, leaving the CMB photons to freely stream. The tiny temperature fluctuations of order $\delta T/T \sim 10^{-5}$, indicated in Fig. 6, reflect the presence of regions with slightly different densities; the wavelength of the photons is red-shifted or blue-shifted depending on the value of the local density. Indeed the properties of the CMB can be time-evolved into a forecast for the Universe that has an excellent match with our observed one.

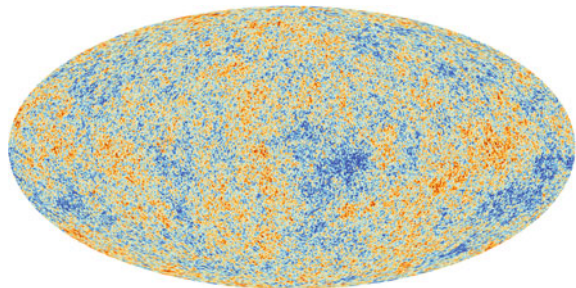
Despite the stunning success of the theory of structure formation, we are left with some puzzling questions: *what set those initial density perturbations? Which is their fundamental origin? Why are they of the same magnitude at any scale? Why were they there at all?*

Surprisingly, inflation suggests a possible answer that is in excellent agreement with observations, thus definitively establishing itself as the leading paradigm for the understanding of the early Universe physics. This answer stems from adding quantum mechanics to the fundamental inflationary dynamics. The scalar field implementation provides once more a very useful stage in order to discuss such a physics. In fact, quantum fluctuations $\delta\phi$ are unavoidable in the homogeneous background represented by $\phi(t)$. These source metric perturbations via the Einstein equations and vice versa according to the following scheme

$$\phi(t, \mathbf{x}) = \phi(t) + \delta\phi(t, \mathbf{x}) \quad \Leftrightarrow \quad g_{\mu\nu}(t, \mathbf{x}) = g_{\mu\nu}(t) + \delta g_{\mu\nu}(t, \mathbf{x}), \quad (33)$$

where $g_{\mu\nu}(t)$ is simply the unperturbed FRW metric, as given by (2). Due to the symmetries and gauge invariance of the coupled system, the resulting physical perturbations reduce to a scalar and a tensor one (vector perturbations decay during the quasi-exponential expansion). Intuitively, quantum fluctuations excite all the light

Fig. 6 The fluctuations of 1 part in 10^5 around the average temperature of $T = 2.73$ of the CMB. Image ESA



particles, in the minimal scenario being the inflaton and the graviton. The scalar perturbations couple to the energy density and eventually lead to the inhomogeneities and anisotropies observed in the CMB. The tensor perturbations are often referred to primordial gravitational waves. They do not couple to the density but induce polarization in the CMB spectrum [10–15]. This is considered to be a unique signature of inflation and many current and proposed experiments are searching for it in the sky.

A detailed treatment of the cosmological perturbations theory goes beyond the aim of the present lecture notes. The interested reader might consult the references [2, 3, 5]. In the following, we would like just to sketch the main consequences of a consistent quantum formulation of the inflationary paradigm. In order to simplify the discussion, we will firstly discuss the pure de Sitter and massless case. In the Sect. 5, we will focus on the proper inflationary analysis, regarded as a small deviation from the case studied here, and eventually extrapolate the significant observational parameters.

4.2 Quantum Scalar Fluctuations During Inflation

Scalar fluctuations can be fully attributed to the quantum nature of the inflaton field living in an unperturbed FRW background. This corresponds to a specific gauge (usually called *spatially flat slicing*) where metric perturbations are set equal to zero. It is a perfectly consistent choice in order to discuss the relevant physics and show how scalar fluctuations behave in an inflationary background metric. The decreasing Hubble radius $(aH)^{-1}$ will play again a crucial role, as we will see.

Let us consider the inflaton field $\phi(t, \mathbf{x})$ with a small spatial dependence as given by (33). The corresponding equation of motion is

$$\ddot{\phi} + 3H\dot{\phi} - \frac{\nabla^2}{a^2}\phi + V' = 0, \quad (34)$$

which differs from the homogeneous equation (27) of the background field $\phi(t)$ for the third extra term. We can Fourier expand the fluctuations such as

$$\delta\phi(t, \mathbf{x}) = \int \frac{d^3\mathbf{k}}{(2\pi)^{3/2}} \delta\phi_{\mathbf{k}}(t) e^{i\mathbf{k}\cdot\mathbf{x}}, \quad (35)$$

with \mathbf{x} and \mathbf{k} being respectively the comoving coordinates and momenta. Note that the Fourier modes $\delta\phi_{\mathbf{k}}$ depend just on the modulo $k = |\mathbf{k}|$ because of the isotropy of the background metric. Then, we can perturb at first order (34), plug the decomposition (35) in and get

$$\delta\ddot{\phi}_{\mathbf{k}} + 3H\delta\dot{\phi}_{\mathbf{k}} + \frac{k^2}{a^2}\delta\phi_{\mathbf{k}} = 0, \quad (36)$$

where we have neglected the additional term $V''\delta\phi_k$ due to the slow-roll conditions (32) during inflation. Equation (36) can be rewritten in a simpler form, without the Hubble friction term, once we introduce the variable

$$v_k \equiv a\delta\phi_k, \quad (37)$$

and switch to conformal time τ . This was defined by (15) and it is naturally related to the comoving Hubble radius as

$$\tau = -\frac{1}{aH}, \quad (38)$$

during a perfect exponential expansion with H constant. Then, the dynamics of the scalar perturbations can be described simply by the equation of a collection of independent harmonic oscillators

$$\boxed{\frac{d^2}{d\tau^2}v_k + \omega_k^2(\tau)v_k = 0}, \quad (39)$$

with time-dependent frequencies

$$\omega_k^2(\tau) = k^2 - \frac{2}{\tau^2} = k^2 - 2(aH)^2. \quad (40)$$

The quantization of the physical system now becomes very easy and one proceeds as in the case of the simple harmonic oscillator, following the canonical procedure. In particular, the modes v_k become nothing but the coefficients of the decomposition of the quantum operator

$$\hat{v}(\tau, \mathbf{k}) = v_k(\tau)\hat{a}_{\mathbf{k}} + v_k^*(\tau)\hat{a}_{\mathbf{k}}^\dagger, \quad (41)$$

where the creation and annihilation operators satisfy the canonical commutation relation

$$\left[\hat{a}_{\mathbf{k}}, \hat{a}_{\mathbf{k}'}^\dagger\right] = \delta^3(\mathbf{k} - \mathbf{k}'). \quad (42)$$

The quantum zero-point fluctuations are given by

$$\langle 0 | \hat{v}^\dagger(\tau, \mathbf{k})\hat{v}(\tau, \mathbf{k}') | 0 \rangle = |v_k(\tau)|^2\delta^3(\mathbf{k} - \mathbf{k}') \quad (43)$$

where the vacuum is defined by $\hat{a}_{\mathbf{k}}|0\rangle = 0$ for any \mathbf{k} . Therefore, computing the quantum perturbations of the inflaton field reduces to solving the classical equation (39) and, then, extracting the time dependence of the Fourier modes $v_k(\tau)$.

The physics of the mode functions v_k , during inflation, is non-trivial and crucially depends on the fact that the comoving Hubble radius shrinks with time. In fact, fluctuations are produced on every scale λ and therefore with any momentum k .

While initially being inside the horizon, they leave the zone of causal physics at one point of the accelerated expansion, as schematically shown in Fig. 4.

One can prove that an exact solution of (39) is

$$v_k(\tau) = \alpha \frac{e^{-ik\tau}}{\sqrt{2k}} \left(1 - \frac{i}{k\tau} \right) + \beta \frac{e^{ik\tau}}{\sqrt{2k}} \left(1 + \frac{i}{k\tau} \right), \tag{44}$$

where α and β are some free parameters to be set by means of the initial conditions. These are defined at very early times, when the relevant scales were still inside the horizon. In the *sub-horizon limit* ($k \ll aH$), that is when $k|\tau| \rightarrow \infty$, the frequencies (40) become time-independent and (39) reduces to

$$\frac{d^2}{d\tau^2} v_k + k^2 v_k = 0, \tag{45}$$

basically the one of a simple harmonic oscillator. We can exploit this fact in order to get the correct normalized solution

$$\lim_{k|\tau| \rightarrow \infty} v_k = \frac{e^{-ik\tau}}{\sqrt{2k}}, \tag{46}$$

which comes from the requirement of a unique vacuum (so-called *Bunch–Davies vacuum*) being the ground state of energy. This sets $\alpha = 1$ and $\beta = 0$ in (44), thus yielding the definitive expression for the Fourier modes

$$\boxed{v_k(\tau) = \frac{e^{-ik\tau}}{\sqrt{2k}} \left(1 - \frac{i}{k\tau} \right)}. \tag{47}$$

Once we have the complete solution (47), we are particularly interested in studying when the modes leave the horizon. We would like indeed to understand how they behave after inflation and affect late time physics. How can quantum fluctuations produced during inflation source density perturbation at CMB decoupling? These events are separated by a huge amount of time where physics is very uncertain. Fortunately, something special happens as we explain below.

The *super-horizon limit* ($k \gg aH$), that is when $k|\tau| \rightarrow 0$, corresponds to the solution

$$\lim_{k|\tau| \rightarrow 0} v_k = -\frac{i}{\sqrt{2}k^{3/2}\tau}. \tag{48}$$

Since the conformal time is related to the scale factor by (15), the latter represents a growing mode $v_k \propto a$, in de Sitter background. Switching to the physical scalar perturbations by means of (37), one obtains that the amplitude $\delta\phi_k$ remains constant as long as the Hubble radius is smaller than their typical length. Modes freeze outside the horizon and this is a crucial result in order to connect the physics of the early Universe to the time when the density perturbations are created. It is a great bonus

we get from inflation as we do not need to worry about the time evolution of such fluctuations for a very substantial part of the cosmic evolution.

Now we can return to (43) and properly evaluate the dimensionless *power spectrum* Δ_v^2 of the quantum fluctuations v_k , defined as

$$\langle 0 | \hat{v}^\dagger(\tau, \mathbf{k}) \hat{v}(\tau, \mathbf{k}') | 0 \rangle \equiv \frac{2\pi^2}{k^3} \Delta_v^2(k) \delta^3(\mathbf{k} - \mathbf{k}'). \quad (49)$$

Then, the power spectrum of the fluctuations after horizon crossing is

$$\lim_{k|\tau| \rightarrow 0} \Delta_v^2(k) = \frac{k^3}{2\pi^2} |v_k|^2 = \left(\frac{aH}{2\pi} \right)^2, \quad (50)$$

where we have used (43) in the first step while (48) and (38) in the last. Therefore, the power spectrum of the physical fluctuations of the inflaton field on super-horizon scales is

$$\Delta_{\delta\phi}^2(k) = \left(\frac{H}{2\pi} \right)^2, \quad (51)$$

which is scale-invariant as no k -dependence enters the expression above. Note that this result was first derived in [16], in a perfect de Sitter approximation, before inflation was proposed. A proper inflationary analysis would bring corrections of order $\mathcal{O}(\varepsilon, \eta)$.

4.3 Classical Curvature and Density Perturbations

In the previous section, we have learned that quantum fluctuations, produced during inflation, stop oscillating once they are stretched to super-horizon scales. Their amplitude freezes at some nonzero value, with scale invariant power spectrum given by (51). This situation lasts for a very long period until the point when the modes re-enter the horizon, during the standard cosmological evolution, as schematically shown in Fig. 4. At horizon re-entry, the amplitude of the modes starts oscillating again inducing the density perturbations. However, the energy density directly interacts with the gravitational potential. Therefore, *how do quantum fluctuations of the inflaton affect the metric curvature and ultimately become density perturbations?* Here, we present a very simple and heuristic derivation, mainly based on the *time-delay formalism* developed in [17].

The presence of quantum fluctuations $\delta\phi(t, \mathbf{x})$ over the smooth background $\phi(t)$ translates into local differences δN of the duration of the inflationary expansion, directly related to curvature perturbations ζ . In fact, not every point in space will end inflation at the same time thus leading to local variations of the scale factor a . Then, fluctuations $\delta\phi$ induce curvature perturbations equal to

$$\zeta = \delta N = H \frac{\delta\phi}{\dot{\phi}} = \frac{\delta a}{a}. \quad (52)$$

The corresponding dimensionless power spectrum is

$$\Delta_\zeta^2(k) = \frac{H^2}{\dot{\phi}^2} \Delta_{\delta\phi}^2(k) = \frac{H^2}{4\pi^2 \dot{\phi}^2}, \quad (53)$$

which, during slow-roll, reads

$$\Delta_\zeta^2 = \frac{1}{12\pi^2} \frac{V^3}{V'^2} = \frac{1}{24\pi^2} \frac{V}{\varepsilon}, \quad (54)$$

where we have used (30) in the first equality and (31) in the second one.

Once inflation ends and the standard cosmological history begins, the energy density will evolve as $\rho = 3H^2$ and, then, decrease as given by (8) (the evolution is shown in Fig. 2). Local delays of the expansion lead to local differences in the density, schematically being $\delta N \sim \delta\rho/\rho$. The amplitude of the density fluctuations will be directly related to the amplitude of the curvature perturbations with power spectrum (54).

4.4 Primordial Gravitational Waves

Primordial quantum fluctuations excite also the graviton, corresponding to tensor perturbations δh of the metric. These have two independent and gauge-invariant degrees of freedom, associated to the polarization components of gravitational waves (usually denoted by h_+ and h_\times). One can prove that the Fourier modes of these functions satisfy an equation analogous to (36). Therefore, one may proceed identically to what done in Sect. 4.2. The dimensionless power spectrum turns out to be

$$\Delta_h^2(k) = 2 \times 4 \times \left(\frac{H}{2\pi} \right)^2, \quad (55)$$

where the factor 2 is due to the two polarizations and the factor 4 is related to different normalization.

5 Observations and Extrapolation

The last 50 years have seen extraordinary success in the development of observational techniques and in the experimental confirmation of our cosmological theories. The discovery of the CMB in 1965 [18] gave the start to a new scientific era where

speculative ideas about the very early Universe have found empirical verification. Analysing this primordial light has become our fundamental tool for the investigation of the very early Universe physics.

Via CMB measurements, we are able to probe the inflationary era and set stringent constraints on the fundamental dynamical mechanism. In the language of the scalar field implementation, we can use observational inputs to impose restrictions on the form of the scalar potential $V(\phi)$. The reason why we are able to have access to such a primordial era is closely connected to the mechanism outlined in the previous section: fluctuations produced during inflation freeze outside the horizon thus providing a link between two very separated moments in time. This situation is depicted in Fig. 7.

In the following, we sketch the basic strategy to extract the inflationary parameters from the CMB data. However, as we will explain, the observational window we have access to is quite small (red region in Fig. 7) and corresponds to a short period around 50–60 e-folds before the end of inflation (this number was derived in Sect. 3 in order to account for the homogeneity and isotropy of the CMB at its largest scale). This implies that different scenarios, with very diverse potentials, may lead to the same observational consequences, as long as they agree in that CMB window. Extrapolating generic predictions, beyond the specific details of the model, and identifying related universality properties will be our primary interest. A description of inflation in terms of the number of e-folds N will turn out to be very useful.

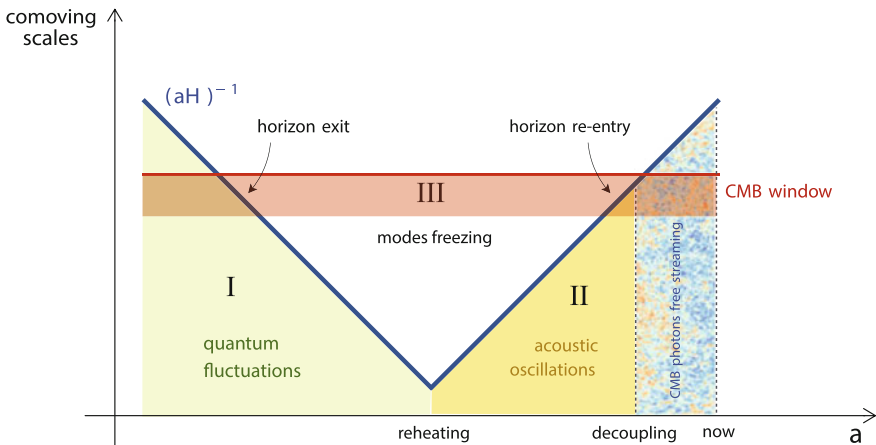


Fig. 7 Quantum fluctuations produced during inflation (*green area*) freeze at the horizon exit. They reenter the horizon after reheating thus sourcing acoustic oscillations of the plasma (*yellow part*). At decoupling time, the CMB photons freely stream towards us who measure their power spectrum just in the small *red window*

5.1 CMB and Inflationary Observables

The CMB is essentially the farthest point we can push our observations to. It is nothing but an almost isotropic 2D surface surrounding us and beyond which nothing can directly reach our telescopes. One can draw an analogy to the surface of the Sun: the inner dense plasma does not allow any light to freely stream outwards and the analysis of the last scattering photons (around 8 min old) becomes essential in order to probe the internal structure. In fact, the homogeneity and isotropy of the CMB together with its tiny and characteristic temperature anisotropy (see Fig. 6) naturally led us to study inflation in Sects. 3 and 4 and consider it as our best probe of what lies beyond that last scattering surface, around 13.4 billions years old.

The power spectrum of the temperature fluctuations in the CMB contains valuable information on the dynamics of inflation. The characteristic shape is simply dictated by the two-point correlation function of the inflaton fluctuations calculated in Sect. 4. A proper investigation of the CMB physics is required in order to understand the functional form, which goes beyond the scope of the present work (see e.g. [2, 19] for a detailed treatment). In practice, it is the so-called *transfer function* which relates the two power spectra: it contains all the information regarding the evolution of the initial fluctuations from the moment when they re-enter the horizon to the time of photon-decoupling (yellow part in Fig. 7) and, subsequently, their projection in the sky as we observe them today. The final result is the solid line of Fig. 8 with the peculiar Doppler peaks originated from the acoustic oscillations of the baryon-photon plasma. The first peak corresponds to a mode that had just time to compress once before decoupling. The other peaks underwent more oscillations and, on small scales, are damped. The high suppression of the power spectrum, at small angular scales, reflects why we are able to probe just a small window of the inflationary era.

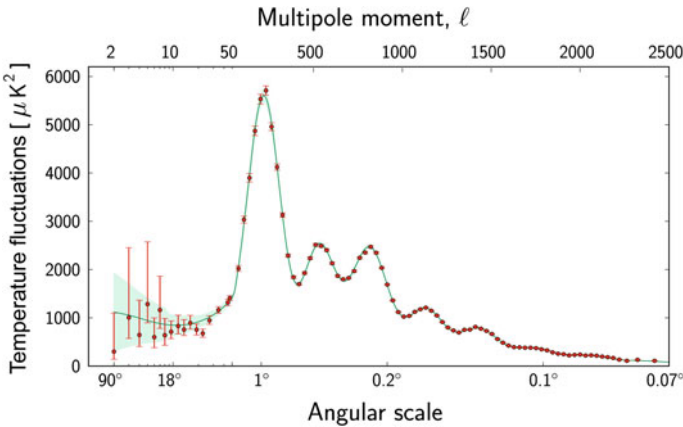


Fig. 8 Power spectrum of the CMB temperature anisotropy as measured by Planck 2015. *Image* ESA

In terms of the number of e-folds this corresponds to about $\Delta N \approx 7$. On the contrary, scales to the left of the first peak show no oscillations as they were superhorizon at the time of decoupling, and hence have not experienced any oscillations.

In Sect. 4, we have derived the power spectrum of perturbations in a perfect de Sitter ($H \approx \text{const}$) and massless ($V'' \approx 0$) approximation. However, an appropriate inflationary analysis would bring some corrections (order slow-roll) and hence a small k -dependence. This is because, during inflation, the energy scale (set by H) will slightly change together with time and the inflaton mass is non-zero, although being very small (order η). In order to parametrize the deviation from scale-invariance, we introduce the *spectral indexes* n_s and n_t defined by

$$n_s - 1 \equiv \frac{d \ln \Delta_\zeta^2}{d \ln k}, \quad n_t \equiv \frac{d \ln \Delta_h^2}{d \ln k}, \quad (56)$$

respectively for scalar and tensor perturbations. In terms of the slow-roll parameters, they read

$$n_s - 1 = 2\eta - 6\varepsilon, \quad n_t = -2\varepsilon. \quad (57)$$

Furthermore, since observations probe just a limited range of k , we can express the deviation from scale-invariance by means of the power laws

$$\Delta_\zeta^2(k) = \Delta_\zeta^2(k_0) \left(\frac{k}{k_0}\right)^{n_s-1}, \quad \Delta_h^2(k) = \Delta_h^2(k_0) \left(\frac{k}{k_0}\right)^{n_t}, \quad (58)$$

where k_0 is a normalization point called *pivot scale*. Note that we have only included the first coefficients of scale-dependence; higher-order effects lead to a scale dependence of these coefficients themselves (referred to as running). Finally, the *tensor-to-scalar ratio* is defined by

$$r \equiv \frac{\Delta_h^2(k_0)}{\Delta_\zeta^2(k_0)} = 16\varepsilon, \quad (59)$$

and indicates the suppression of the power of tensor with respect to scalar modes.

5.2 Planck Data

The Planck satellite [20, 21] has mapped the Universe with unprecedented accuracy. In this way it has set stringent constraints on the parameters related to the inflationary dynamics. First of all, at $k_0 = 0.05 \text{ Mpc}^{-1}$, the experimental value for the scalar amplitude (first detected by COBE [22]) is

$$\Delta_\zeta^2(k_0) = (2.14 \pm 0.10) \times 10^{-9}. \quad (60)$$

Secondly, the deviation from perfect scale-invariance has been definitively confirmed and the scalar spectral index n_s has been measured to be

$$n_s = 0.968 \pm 0.006. \tag{61}$$

On the other hand, the value of the tensor-to-scalar ratio has been observationally bounded to be

$$r < 0.11. \tag{62}$$

These values can be read from Fig. 12 of [21] where Planck 2015 results for the spectral index and tensor-to-scalar ratio with the predictions of different inflationary models are superimposed.

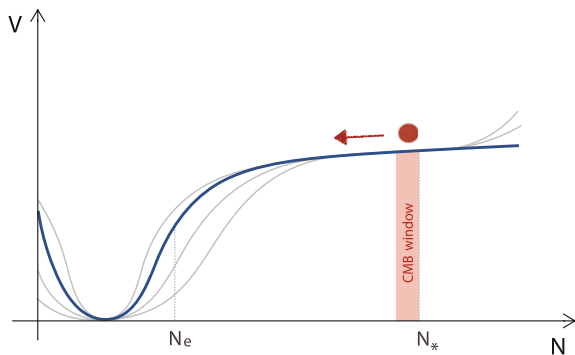
5.3 Universality at Large- N

As we saw in Sect. 5.1, the window we can probe by means of CMB observations corresponds to a small portion of the inflationary trajectory. The measured values of the cosmological parameters (61) and (62) constrain the form of the scalar potential just on a limited part. This sensitive region is located around 50–60 e-folds before the end of inflation, when the modes relevant for the CMB power spectrum left the region of causal physics. The practical situation is that several scenarios can give rise to the same predictions despite the details of specific model. This situation is visually explained in Fig. 9.

In Sect. 3, we have described the inflationary background dynamics in terms of the canonical normalized field ϕ . A valid alternative description is the one in terms of the number of e-folds N , provided the relation

$$\frac{d\phi}{dN} = \sqrt{2\varepsilon}. \tag{63}$$

Fig. 9 Cartoon of a typical inflationary scalar potential (blue line) with different deviation (grey lines). The details of the models are different but they agree on the CMB window thus yielding identical observational predictions



This can be interpreted as a background field redefinition from ϕ , with canonical kinetic terms, to the field N with Lagrangian

$$\mathcal{L} = \sqrt{-g} \left[\frac{1}{2} R - \varepsilon(N) (\partial N)^2 - V(N) \right]. \quad (64)$$

Once switched to the N -formulation, we can expand the cosmological variables at large number of e-folds N , in order to keep the relevant features for observations. This approach is also motivated by the percentage-level deviation of the Planck reported value for the spectral index (61) from unity which can be interpreted as

$$n_s = 1 - \frac{2}{N}, \quad (65)$$

with N being equal to the number of e-folds between the points N_* of horizon crossing and N_e where inflation ends, that is

$$N = N_* - N_e. \quad (66)$$

These arguments naturally lead to assume the first slow-roll parameter scaling as [23–25]

$$\varepsilon = \frac{\beta}{N^p}, \quad (67)$$

where β and p are constant and we have neglected higher-order terms in $1/N$ as not relevant for observations. This simple assumption (67) yields to

$$r = \frac{16\beta}{N^p}, \quad n_s = \begin{cases} 1 - \frac{2\beta+1}{N}, & p = 1, \\ 1 - \frac{p}{N}, & p > 1, \end{cases} \quad (68)$$

where we have discarded the case $p < 1$ as it generically not compatible with the current cosmological data.

The analysis at large- N allows us to identify the generic predictions of the cosmological scenarios with a first slow-roll parameter scaling as (67) (implications on the inflaton excursion $\Delta\phi$ studied in [26, 27]). Most of the inflationary models in literature have this property and many examples are listed in [24, 25]. Specifically, by means of (68), we can exclude a consistent region of the (n_s, r) plane and make definite predictions for our cosmological variables [24, 28]. The allowed regions can be seen in Fig. 1 of [24] where are shown the predictions of the inflationary scenarios with equation of state parameter given by (67) superimposed over the Planck data. Given the favored value of the spectral index (65), one has generically a forbidden region for value of the tensor-to-scalar ratio r . In particular, given the best fit value for n_s and the strict bound on r , we will generically expect a very low value for the tensor-to-scalar ratio, probably order 10^{-3} .

6 Inflation, Supergravity and Attractors

In the last chapter of these lecture notes, we change gears somewhat and will discuss a more theoretical underpinning of inflationary models. In particular, we consider inflation in the context of supersymmetry. Due to the presence of gravity, this naturally implies the framework of supergravity [29]. Although not observed (yet) at the energies of particle colliders, i.e. up to 1 TeV, supersymmetry is a natural ingredient of many theories of UV physics such as string theory. Given that inflation takes place at far higher energies than the Standard Model, this appears as a theoretically natural framework. Moreover, supersymmetry helps in protecting the inflaton mass from a very large contribution which would render inflation inviable: the inflaton mass is protected from being raised above the Hubble scale. This reduces the amount of necessary finetuning/modelbuilding by a few orders of magnitude. Finally, supergravity naturally includes (many) scalar fields, yielding a magnitude of possible inflaton candidates. In this chapter we will address the type of scalar potentials that arise (or can be embedded) in this set of theories, and extract inflationary predictions from these.

6.1 Flat Kähler Geometry

We will start from the simplest possible supergravity models, with $\mathcal{N} = 1$ and a single superfield Φ . Moreover, we take a flat geometry for this superfield: it is given by $ds^2 = d\Phi d\bar{\Phi}$. Note that it has an $ISO(2)$ isometry group. We will assume that inflation proceeds along the real part of Φ , which is one of the isometry directions. The canonical Kähler potential reads

$$K = \Phi \bar{\Phi}. \quad (69)$$

However, the scalar potential will be of the form $V = e^K \times \dots$, where the dots are determined by the superpotential. For generic choices of the latter, the present Kähler potential will therefore induce order-one contributions to the second slow-roll parameter η of inflation [30]. The reason for this is the particular choice of Kähler potential: it has a rotational invariance but breaks the translational symmetry along the inflationary direction.

To remedy this, one can invoke a Kähler transformation

$$K \rightarrow K + \lambda + \bar{\lambda}, \quad W \rightarrow e^{-\lambda} W, \quad (70)$$

with holomorphic parameter λ , which leaves the entire $\mathcal{N} = 1$ theory invariant. A bringsbrins one to [31]

$$K = -\frac{1}{2}(\Phi - \bar{\Phi})^2, \quad (71)$$

which does respect the shift symmetry of the inflaton. As a consequence, the scalar potential does not receive order-one contributions from the Kähler potential: we have evaded the η -problem. Additional simplifications arise as both K and its first derivative K_ϕ vanish along the real inflationary direction.

In this simple set-up with a single superfield, one can introduce a superpotential

$$W = f(\Phi). \quad (72)$$

Provided the function f is a real holomorphic function, it is consistent to truncate to the real part of Φ . We have therefore succeeded in identifying a possible single-field inflationary trajectory. However, its scalar potential reads

$$V = -3f(\Phi)^2 + f'(\Phi)^2, \quad (73)$$

which makes it difficult to realize e.g. the simplest inflationary model with a quadratic scalar potential in this set-up.

At this point we will follow [31] and extend the field content. In addition to the chiral superfield Φ that contains the inflaton, we introduce a second superfield S . Its role will be to “soak up” the effects of supersymmetry breaking, leaving no constraints on the inflationary potential. Indeed we will see that one can introduce arbitrary inflationary models in this way [32].

The two-superfield model reads

$$K = -\frac{1}{2}(\Phi - \bar{\Phi})^2 + S\bar{S}, \quad W = Sf(\Phi), \quad (74)$$

where we have added an additional piece to the Kähler potential, and moreover we have assumed that the superpotential is linear in the new field S . As inflation will take place along $\Phi - \bar{\Phi} = S = 0$, the F-term contributions read

$$D_\phi W = 0, \quad D_S W = f, \quad (75)$$

confirming that indeed supersymmetry breaking takes place in the S -superfield. Since both K and W vanish during inflation, the potential is given by

$$V = f(\phi)^2, \quad (76)$$

where ϕ is the real part of Φ . At this point one can choose $f = m\Phi$ in the original superpotential, thus reproducing the quadratic inflationary potential from a supergravity theory. This was the original motivation and result of [31]. However, as was pointed out in [32], the same set-up allows for arbitrary real functions $f(\Phi)$. This shows that one can build an arbitrary scalar potential in this simple scenario. This implies that the predictive power of supergravity is rather limited! However, we will see in the next subsection that this conclusion changes dramatically when including curvature.

6.2 Hyperbolic Kähler Geometry and α -Attractors

Instead of a flat geometry, we now turn to the other maximally symmetric possibility. This is the hyperbolic space of the Poincaré half-plane (or disc). We will use half-plane coordinates with $Re(\Phi) > 0$. In this case the metric takes the form

$$ds^2 = 3\alpha \frac{d\Phi d\bar{\Phi}}{(\Phi + \bar{\Phi})^2}, \tag{77}$$

whose curvature is given by

$$R_K = -\frac{2}{3\alpha}. \tag{78}$$

Note that it is negative (corresponding to hyperbolic space), and maximal symmetry implies it to be constant over moduli space. Its isometries are given by the Möbius group, which contain

- Nilpotent symmetry: $\Phi \rightarrow \Phi + ic$, corresponding to a vertical shift,
- Non-compact symmetry: $\Phi \rightarrow e^\lambda \Phi$, corresponding to a horizontal shift,
- Compact symmetry with a more complicated action.

The usual Kähler potential for this space is given by

$$K = -3\alpha \log(\Phi + \bar{\Phi}). \tag{79}$$

Note that it breaks all but one of the isometries: it is only invariant under the nilpotent generator. Therefore it is not invariant under shifts of the inflaton, which again we will take along the real axis of Φ . Similar to the flat case, one can however do a Kähler transformation to make this isometry explicit in the Kähler potential. In this case one finds [33]

$$K = -3\alpha \log \left[\frac{\Phi + \bar{\Phi}}{(\Phi \bar{\Phi})^{1/2}} \right], \tag{80}$$

which is invariant under the non-compact generator. Again both K and K_ϕ vanish along the inflationary trajectory. This therefore seems to be the most natural starting point for our discussion of the curved case.

Inclusion of the supersymmetry breaking sector leads to

$$K = -3\alpha \log \left[\frac{\Phi + \bar{\Phi}}{(\Phi \bar{\Phi})^{1/2}} \right] + S\bar{S}, \tag{81}$$

while we retain the simple superpotential of the flat case:

$$W = Sf(\Phi). \quad (82)$$

Again this allows us to restrict to the real axis of Φ : the truncation to $\Phi - \bar{\Phi} = S = 0$ is consistent provided the function f is real. The single-field inflationary potential in this case reads

$$V = f^2 \left(e^{-\sqrt{\frac{2}{3\alpha}}\varphi} \right), \quad (83)$$

where φ is the canonically normalized scalar field that is related to the real part of the superfield Φ by

$$\phi = e^{-\sqrt{\frac{2}{3\alpha}}\varphi}. \quad (84)$$

Note that the curvature has a dramatic effect on the inflationary potential: the argument of the arbitrary function f is now given by an exponential of the inflaton. For a generic function f that, when expanded around $\phi = 0$, has a non-vanishing value and a slope, the resulting inflationary potential reads

$$V = V_0(1 - e^{-\sqrt{\frac{2}{3\alpha}}\varphi} + \dots). \quad (85)$$

The potential therefore attains a plateau at infinite values of φ and has a specific exponential drop-off at finite values. At smaller values of φ , higher-order terms will come in whose form depends on the details of the function f . However, when restricting to order-one values of α , none of these higher-order terms are important for inflationary predictions: in order to calculate observables at $N = 60$, one only needs the leading term in this expansion. This means that all dependence of the function f has dropped out: the only remaining freedom is the parameter α .

In more detail, the inflationary predictions of this model are given by

$$n_s = 1 - \frac{2}{N} + \dots, \quad r = \frac{12\alpha}{N^2} + \dots. \quad (86)$$

The dots indicate higher-order terms in $1/N$, whose coefficients depend on the details of the function f ; however, at $N \sim 60$, none of these higher-order terms are relevant for observations. The leading terms are independent of the functional freedom and only depend on the curvature of the manifold. This is what is referred to as α -attractors [34–40]: as α varies from infinity (i.e. the flat case) to order one or smaller, the inflationary predictions go from completely arbitrary (in the flat case) to the very specific values above. Turning on the curvature therefore “pulls” all inflationary models into the Planck dome in the (n_s, r) plane. The specific predictions include the magnitude of the tensor-to-scalar ratio, which naturally comes out at the permille level, as well as the scale dependence of the spectral index of scalar perturbations:

this is referred to as the running parameter, and takes the expression

$$\alpha_s = -\frac{d}{dN}n_s = -\frac{2}{N^2} + \dots. \quad (87)$$

Future observations will hopefully shed light on these crucial inflationary observables, and thus can (dis)prove the α -attractors framework.

7 Discussion

The topic of these lecture notes has been dual: both to provide the reader with an understanding of recent CMB observations, as well as a theoretical proposal to explain these data. We hope to have given a flavour of the excitement on the present status of observations and the theoretical expectations for possible future observations. First and foremost amongst the latter are tensor perturbations: a crucial signature of inflation, a detection of these would prove the quantum-mechanical nature of gravity as well as provide the inflationary energy scale. Moreover, depending on its value, such a detection would either disprove or lend further evidence to the inflationary models known as α -attractors.

Acknowledgments We are grateful to our collaborators John Joseph Carrasco, Mario Galante, Juan Garcia-Bellido, Renata Kallosh and Andrei Linde, who have all contributed in a major way to the results described in the last chapters. Moreover, DR would like to thank the organization of the school on “Theoretical Frontiers in Black Holes and Cosmology” in Natal, Brasil, from June 8 to 12, 2015, for a stimulating atmosphere.

References

1. A.D. Linde, Particle physics and inflationary cosmology. *Contemp. Concepts Phys.* **5**, 1 (1990). [arXiv:hep-th/0503203](https://arxiv.org/abs/hep-th/0503203)
2. S. Dodelson, *Modern Cosmology* (Academic Press, Amsterdam, 2003)
3. V. Mukhanov, *Physical Foundations of Cosmology* (Cambridge University Press, Oxford, 2005)
4. S. Weinberg, *Cosmology* (Oxford University Press, Oxford, 2008)
5. D. Baumann, Inflation, in *Physics of the large and the small, TASI 09, proceedings of the Theoretical Advanced Study Institute in Elementary Particle Physics, Boulder, Colorado, USA, 1–26 June 2009* (2011) pp. 523-686, [arXiv:0907.5424](https://arxiv.org/abs/0907.5424) [hep-th]
6. E. Hubble, A relation between distance and radial velocity among extra-galactic nebulae. *Proc. Natl. Acad. Sci.* **15**, 168 (1929)
7. A.H. Guth, The inflationary universe: a possible solution to the horizon and flatness problems. *Phys. Rev. D* **23**, 347 (1981)
8. A.D. Linde, A new inflationary universe scenario: a possible solution of the horizon, flatness, homogeneity, isotropy and primordial monopole problems. *Phys. Lett. B* **108**, 389 (1982)
9. A. Albrecht, P.J. Steinhardt, Cosmology for grand unified theories with radiatively induced symmetry breaking. *Phys. Rev. Lett.* **48**, 1220 (1982)

10. U. Seljak, Measuring polarization in cosmic microwave background. *Astrophys. J.* **482**, 6 (1997). [arXiv:astro-ph/9608131](#)
11. M. Kamionkowski, A. Kosowsky, A. Stebbins, A Probe of primordial gravity waves and vorticity. *Phys. Rev. Lett.* **78**, 2058 (1997). [arXiv:astro-ph/9609132](#)
12. U. Seljak, M. Zaldarriaga, Signature of gravity waves in polarization of the microwave background. *Phys. Rev. Lett.* **78**, 2054 (1997). [arXiv:astro-ph/9609169](#)
13. M. Zaldarriaga, U. Seljak, An all sky analysis of polarization in the microwave background. *Phys. Rev. D* **55**, 1830 (1997). [arXiv:astro-ph/9609170](#)
14. M. Kamionkowski, A. Kosowsky, A. Stebbins, Statistics of cosmic microwave background polarization. *Phys. Rev. D* **55**, 7368 (1997). [arXiv:astro-ph/9611125](#)
15. W. Hu, M.J. White, A CMB polarization primer. *New Astron.* **2**, 323 (1997). [arXiv:astro-ph/9706147](#)
16. T.S. Bunch, P.C.W. Davies, Quantum field theory in de sitter space: renormalization by point splitting. *Proc. R. Soc. Lond. A* **360**, 117 (1978)
17. A.H. Guth, S.Y. Pi, Fluctuations in the new inflationary universe. *Phys. Rev. Lett.* **49**, 1110 (1982)
18. A.A. Penzias, R.W. Wilson, A measurement of excess antenna temperature at 4080-Mc/s. *Astrophys. J.* **142**, 419 (1965)
19. W. Hu, Lecture Notes on CMB Theory: From Nucleosynthesis to Recombination. [arXiv:0802.3688](#) [astro-ph]
20. P.A.R. Ade et al., Planck Collaboration, Planck 2015 results. XIII. Cosmological parameters. [arXiv:1502.01589](#) [astro-ph.CO]
21. P.A.R. Ade et al., Planck Collaboration, Planck 2015 results. XX. Constraints on inflation. [arXiv:1502.02114](#) [astro-ph.CO]
22. G.F. Smoot et al., Structure in the COBE differential microwave radiometer first year maps. *Astrophys. J.* **396**, L1 (1992)
23. V. Mukhanov, Quantum cosmological perturbations: predictions and observations. *Eur. Phys. J. C* **73**, 2486 (2013) [arXiv:1303.3925](#) [astro-ph.CO]
24. D. Roest, Universality classes of inflation. *JCAP* **1401**, 007 (2014). [arXiv:1309.1285](#) [hep-th]
25. J. Garcia-Bellido, D. Roest, Large- N running of the spectral index of inflation. *Phys. Rev. D* **89**(10), 103527 (2014) [arXiv:1402.2059](#) [astro-ph.CO]
26. J. Garcia-Bellido, D. Roest, M. Scalisi, I. Zavala, Can CMB data constrain the inflationary field range? *JCAP* **1409**, 006 (2014). [arXiv:1405.7399](#) [hep-th]
27. J. Garcia-Bellido, D. Roest, M. Scalisi, I. Zavala, Lyth bound of inflation with a tilt. *Phys. Rev. D* **90**(12), 123539 (2014). [arXiv:1408.6839](#) [hep-th]
28. P. Creminelli, S. Dubovsky, D.L. Nacir, M. Simonovic, G. Trevisan, G. Villadoro, M. Zaldarriaga, Implications of the scalar tilt for the tensor-to-scalar ratio. [arXiv:1412.0678](#) [astro-ph.CO]
29. D.Z. Freedman, A. Van Proeyen, *Supergravity* (Cambridge University Press, Cambridge, 2012)
30. E.J. Copeland, A.R. Liddle, D.H. Lyth, E.D. Stewart, D. Wands, False vacuum inflation with Einstein gravity. *Phys. Rev. D* **49**, 6410 (1994). [arXiv:astro-ph/9401011](#)
31. M. Kawasaki, M. Yamaguchi, T. Yanagida, Natural chaotic inflation in supergravity. *Phys. Rev. Lett.* **85**, 3572 (2000). [arXiv:hep-ph/0004243](#)
32. R. Kallosh, A. Linde, T. Rube, General inflaton potentials in supergravity. *Phys. Rev. D* **83**, 043507 (2011). [arXiv:1011.5945](#) [hep-th]
33. J.J.M. Carrasco, R. Kallosh, A. Linde, D. Roest, Hyperbolic geometry of cosmological attractors. *Phys. Rev. D* **92**(4), 041301 (2015). [arXiv:1504.05557](#) [hep-th]
34. R. Kallosh, A. Linde, Universality class in conformal inflation. *JCAP* **1307**, 002 (2013). [arXiv:1306.5220](#) [hep-th]
35. S. Ferrara, R. Kallosh, A. Linde, M. Porrati, Minimal supergravity models of inflation. *Phys. Rev. D* **88**(8), 085038 (2013). [arXiv:1307.7696](#) [hep-th]
36. R. Kallosh, A. Linde, D. Roest, Superconformal inflationary α -attractors. *JHEP* **1311**, 198 (2013). [arXiv:1311.0472](#) [hep-th]
37. R. Kallosh, A. Linde, D. Roest, Large field inflation and double α -attractors. *JHEP* **1408**, 052 (2014). [arXiv:1405.3646](#) [hep-th]

38. M. Galante, R. Kallosh, A. Linde, D. Roest, Unity of cosmological inflation attractors. *Phys. Rev. Lett.* **114**(14), 141302 (2015). [arXiv:1412.3797](#) [hep-th]
39. D. Roest, M. Scalisi, Cosmological attractors from a-scale supergravity. *Phys. Rev. D* **92**, 043525 (2015). [arXiv:1503.07909](#) [hep-th]
40. M. Scalisi, Cosmological α -Attractors and de Sitter Landscape. [arXiv:1506.01368](#) [hep-th]